Towards an Optimization of DOD Printing of Complex Fluids

Moussa Tembely[1], Damien Vadillo[2], Malcolm R. Mackley[2] and Arthur Soucemarianadin[1]
[1] UJF-Grenoble 1 / Grenoble-INP / CNRS, LEGI UMR 5519, Grenoble, F-38041, France
[2] Department of Chemical Engineering and Biotechnology, University of Cambridge, Cambridge CB2 3RA, United Kingdom

Abstract

The present work deals with the study of drop formation of polymeric fluids with the objective of providing a correlation between fluid printability and its rheological properties. An innovative approach combining together many experiments and numerical simulations of free surface flows is proposed. Viscoelasticity of fluids is probed using experimental methods that give access to the frequency, strain and strain rate domains of the drop on demand jetting process. High frequency viscoelastic measurements are performed using a Piezo Axial Vibrator (PAV) that enables linear viscoelastic measurements (LVE) to be obtained in the range 1Hz - 10 kHz. Non linear viscoelastic (NLVE) measurements are performed using the "Cambridge Trimaster", a filament stretching apparatus that enables nonlinear stretching and filament break up to be observed at strains similar to that found in DOD. A series of low viscosity fluids possessing similar shear properties but differing by their elastic properties are used in this study. Polymer addition is found to develop fluid viscoelasticity and, in particular, an increase in the relaxation times at large strain extensional flows. Besides these different experiments, a numerical investigation of the stretching process is also performed with the development of a one-dimensional model coupled with the Arbitrary Lagrangian Eulerian (ALE) formulation. After preliminary comparison for the Newtonian case, the polymers solutions are modeled using FENE-CR constitutive equations. The predicted diameter of the middle of the thinning filament is compared against measurements obtained with the "Cambridge Trimaster" and a good agreement is found. The dynamics of drop formation and pinch-off of the above mentioned fluids are further investigated using pendant drop formation from a nozzle under the influence of gravity. The same one-dimensional model, with parameters obtained from filament thinning, is used to model the faucet phenomenon. Transient lengths and diameters of filaments are compared with experimental measurements and demonstrate the close resemblance between the two processes although the filament stretching and thinning is more controllable and allows to have access to higher Hencky strains as compared to the pendant drop technique. The ability to model the fluids in two very different flow situations allow to predict their behavior in a drop on demand process and to propose an optimization of the printing process through the use of appropriate dimensionless numbers.

Introduction

For already some time now, ink-jet printing has been expanded into a versatile method for deposition of minute quantities of materials in various industrial manufacturing processes. As such, it is a key technology for controlled polymer deposition in relation to fabrication of multicolor polymer light emitting diode (pLED) displays and other polymer based electronic parts, ceramics, biopolymer arrays etc. The polymeric additives profoundly influence fluid rheological properties hence leading to novel applications in industry. Several of these applications are based on the coil-stretch transition and subsequent stretching of polymer coils in elongational flows followed by an enhancement of elongational viscosity. Moreover, many fluids of interest to lab-on-a-chip devices are likely to exhibit complex micro-structure and non-Newtonian properties, such as viscoelasticity. In fact, given the small geometrical length scales, one expects these effects to be accentuated in micro-devices. Therefore the understanding of non-Newtonian rheological behavior such as elasticity is of both fundamental and practical importance [1].

In this paper, we investigate the effects of polymer addition and concentration on fluid filament thinning and drop break-up in various situations. Elasticity effects are examined using dilute polymeric solutions. The results obtained for the polymeric fluids are compared to those for a viscous Newtonian fluid. The viscosity and modulii measurements in the linear viscoelastic regime are obtained using the Piezo Axial Vibrator device. The elongational properties in the non linear viscoelastic regime are first obtained using the "Cambridge Trimaster" device which stretches a small amount of fluid attached between two identical pistons. Filament thinning follows once the pistons are stopped. This apparatus has been especially designed to characterize low viscosity inkjet fluids where both the capillary thinning and break-up could be measured with time transients lower than a few milliseconds. As shown elsewhere [2], the elasto-capillary times are found to differ from those in the LVE regime by two orders of magnitude. The dynamics of drop formation and pinch-off are then investigated through filament rupture from a nozzle under the influence of gravity alone using the pendant drop technique. It is shown here that a one-dimensional (1D) model based on simplification of the governing 2D system through the use of the slender-jet approximation captures well the physics of filament thinning and drop formation even in situations of a finite flow rate where the relative importance of inertial to capillary force, on the dynamics is varied. It is demonstrated that the addition of polymer has a profound influence in retarding the break-up dynamics resulting in higher extensional viscosity and relaxation time and proving to be more effective in stabilizing the filament.

The good agreement of the 1-D model with thinning and pendant drop measurements allows using it to predict the dynamics of filament formation and pinch-off in the case of DOD. As a conclusion of this study, a printability criterion is proposed taking into account non-Newtonian fluid dynamics.

Experimental

In this section, the fluids and the experimental methods used in this work are examined in some detail.

Fluids

Solutions of polystyrene with molecular weight of 110 kg/mol (PS110) dissolved in mixtures of diethyl phthalate (DEP) and dioctyl phthalate (DOP) were prepared. The ratio between DEP and DOP was adjusted in order to match the fluids complex viscosity at a value of about 19mPa.s at 25°C. A mixture of PS110 in DEP at higher concentration, namely 2.5wt%, is also formulated. The fluid physical properties are summarized in Table 1 with surface tension and density of the solutions estimated from weight ratio DEP/DOP.

Fluid	M_w (kg/kmol)	DEP (w/w)	c (wt%)	ρ (kg/m^3)	σ (mN/m)	η_0 (mPa.s)
I		67	0	1076	35	19.6
II	110000	72	0.2	1083	35	19
III	110000	77	0.5	1089	36	20
IV	110000	100	2.5	1120	37	27

***Table 1**. Fluids physical parameters.*

Linear viscoelastic measurements

The high frequency linear viscoelasticity (LVE) behavior of the fluids was investigated using a Piezo Axial Vibrator (PAV) [3]. The range of frequency of this device is well above that covered in DOD printing so the measurements are representative of operating conditions. The PAV gives the shear modulus, $G^* = G' + iG''$, and the complex viscosity $\eta^* = G^*/i\omega$ (where ω is in rad/s). The temperature is regulated in the device and a range of temperatures situated between 5°C and 50°C can be investigated. It is to be noted that the elastic modulus G' of fluid III is above that of fluid II whilst the loss modulus is more or less the same (Fig.1a). The complex viscosity is constant irrespective of frequency and is similar for all three fluids (Fig.1b).

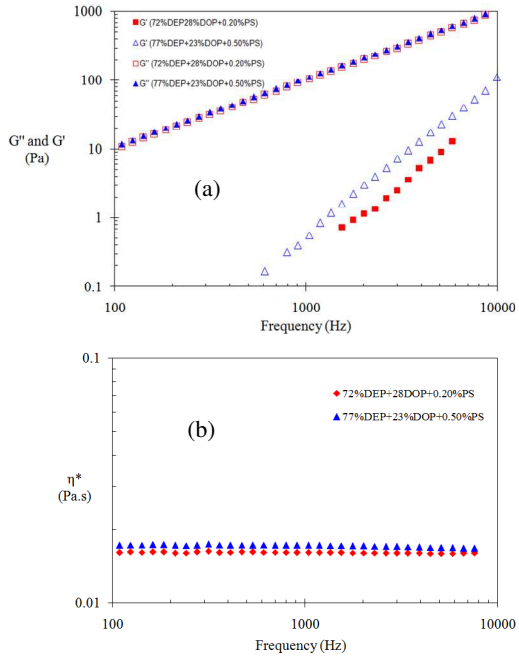

***Figure 1.** Plots of (a) storage G', loss modulus G" and (b) complex viscosity measured using PAV for fluids II and III.*

Non-linear viscoelastic measurements

Filament thinning

The second experimental set up is a filament stretching, extensional rheometer, the "Cambridge Trimaster" [4]. This apparatus performs filament stretching at a constant velocity for a fluid initially placed between two pistons of initial diameter D_0=1.2mm (Fig.2).

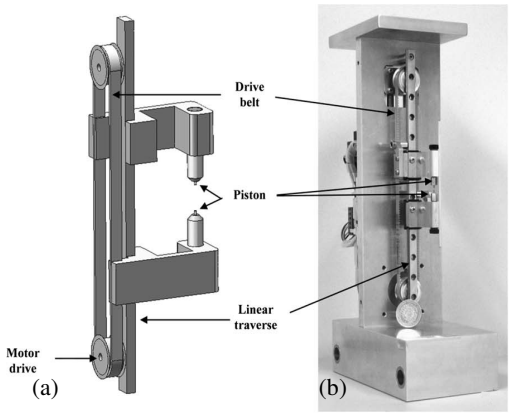

***Figure 2.** "Cambridge Trimaster" filament stretching and breakup apparatus (a) schematic (b) photograph.*

Both pistons are attached on the opposite side of a belt and move symmetrically apart for a given distance allowing the mid-filament to remain in a central position during the experiment. The pistons can be moved from a distance of 10μm to 10cm at a maximum relative velocity of 1m/s. When the pistons stop, the filament self-thins under the action of capillary and viscous forces. The Bond number was calculated to be small ($Bo = \rho g D_0^2/4\sigma = 0.1$), confirming that gravitation effects were negligible in comparison to capillary forces.

A high speed camera (Photron Fastcam 1024 PCI) was coupled with the "Cambridge Trimaster", allowing the transient profiles to be recorded at a frame rate of 45000 frames per second at a resolution of 64x128 pixels, and with a shutter time as low as 3μs. The filament thinning measurements as well as the filament break-up behavior were obtained using automatic image processing specifically developed for, and included within, the "Cambridge Trimaster" software package. This apparatus enables the measurement of the transient elongational viscosity and the observation of filament profiles. Both elements are relevant to inkjet drop and satellite formation.

Pendant droplet

A third set of experiments is related to pendant droplet measurements. This method consists in forming a droplet at the end of a well sized tube (inner diameter of 150 μm and external diameter of 310μm) by slowly increasing the fluid volume using a syringe pump. Initially, quasistatic equilibrium between surface tension and gravity maintains the droplet of radius R_0 attached to the tube if $\rho g R_0^2/3\sigma \leq 1$. When droplet weight overcomes surface tension forces, gravity initiates the break-up and performs an axial

stretch of the liquid located in the break-up region. A cylinder of fluid is subsequently created and thins under the conjugated action of gravity and surface tension whereas viscoelastic forces acts against this mechanism (Fig. 3). Similar imaging techniques as the one used for filament stretching and thinning experiments have proved to be useful to record the liquid faucet process with higher accuracy than previous measurement reported in the literature [5].

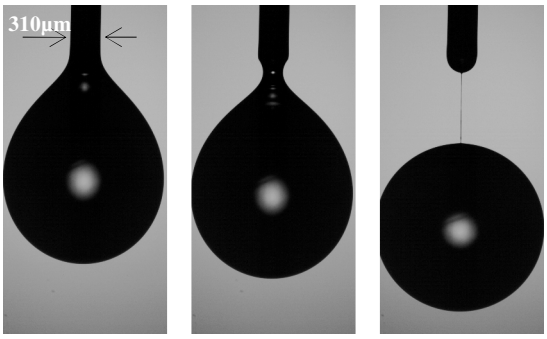

Figure 3. *Sequence of images describing the pendant droplet experiment.*

Modeling

Slender body approximation

Filament stretching and pendant drop configurations have been extensively studied both experimentally and numerically. The modeling of these free-surface flows represents a complicated and computationally challenging task, thus the rationale of a simple model given in this paper to address the different cases.

The radius of the filament $h(z, t)$ is assumed to vary slowly along the liquid jet and considering only the leading-order approximation in an expansion in the radius, the conservation of mass and momentum equation leads to the following nonlinear one-dimensional equations describing the filament dynamics [2, 6, 7]:

$$\partial_t h + vh' + v'h/2 = 0 \tag{1}$$

$$\partial_t v + vv' = -\kappa' + 3Oh\frac{(v'h^2)'}{h^2} + \frac{1}{h^2}\left[h^2(\sigma_{zz}-\sigma_{rr})\right]' + \mathrm{Bo} \tag{2}$$

where the prime denotes the derivative with respect to z coordinates.

The dimensionless form is deduced using R_0, the radius of the capillary, as a characteristic length scale whilst the capillary time scale $\tau = (\rho R^3/\sigma)^{1/2}$ is used as the time scale. Thus the resulting drop dimensionless groups are the Ohnesorge number $Oh=\mu/(\rho R_0\sigma)^{1/2}$ and the gravitational Bond number $\mathrm{Bo} = \rho g R_0^2/\sigma$.

To avoid instability in the solution and gain the complete ability to represent a rounded drop, the full expression of the curvature given in equation (14) is taken [6]. This is not asymptotically correct as shown in [8] but this choice has been justified and used by many authors [6, 9]. The radial expansion requires replacing the mean curvature by the leading-order expression $1/h$ alone, but the applicability of the equations is improved by accounting for the full curvature, since the equations retrieve a spherical drop among the equilibrium solutions:

$$\kappa = \frac{1}{h(1+h'^2)^{1/2}} - \frac{h''}{(1+h'^2)^{3/2}} \tag{3}$$

The extra-stress expression is deduced through the use of the non-Newtonian constitutive equation to be detailed later.

To apply the previous equations special treatment of the boundary conditions has to be carried out in order to address both the filament thinning and the pendant drop configurations. The Arbitrary Lagrangian-Eulerian (ALE) technique was used to handle the dynamics of the boundaries with a moving grid where the new mesh coordinates are computed based on the motion of the boundaries of the structure. The governing equations are solved using these moving coordinates. The model, as presented here, has the additional advantage of not needing any un-physical artificial viscosity just for the purpose of pinning the fluid at the piston as required in [7] or any approximation to properly handle the pendant drop tip singularly. These boundary conditions using ALE techniques are detailed below.

Stretching

In the stretching configuration, no-slip conditions are imposed at the piston surfaces:

$$h(z=-L/2,t) = h(z=L/2,t) = R_0 \tag{4}$$

$$v(z=-L/2,t) = -V_p,\ v(z=L/2,t) = V_p \tag{5}$$

where V_p is the stretching velocity applied to the pistons, and L the time-dependent filament length.

Pendant drop

The way the drop tip is handled here is a characteristic of our one-dimensional ALE formulation and is in contrast to others reported in the literature, where either an undefined boundary condition is given or polynomial interpolations are made. Furthermore an extension accounting for non-Newtonian behavior is also given here. The previous equations (1-2) are subject to boundary conditions of the type plug flow.

At the nozzle exit we have:

$$h(z=0,t) = 1 \tag{6}$$

$$v(z=0,t) = U_f \tag{7}$$

and the dimensionless inflow velocity $Ua = U_f\,\tau/R_0 = We^{1/2}$ where the Weber number, $We=\rho R_0 U_f^2/\sigma$.

The drop tip velocity corresponds to the time rate of change of the length $L(t)$ of the drop through the ALE formulation, hence:

$$h(z=L(t),t) = 0 \tag{8}$$

$$v(z=L(t),t) = \frac{dL(t)}{dt} \tag{9}$$

As the initial condition for the shape of the jet, we used a hemispherical droplet described by $h(z, t=0)=(1-z^2)^{1/2}$. With these different ingredients a thorough quantitative evaluation of a 1-D model of drop formation from a pendant drop configuration based on the slender jet approximation can be carried out. This is done in the next section.

Non-Newtonian Model: 1D FENE-CR

Numerical simulations of non-Newtonian thinning filament and pendant drop configurations are carried out by solving the Navier-Stokes equations within the lubrication approximation as given by the equations (1)-(9).

In order to establish the non-Newtonian 1-D model description, the previous equations are completed by expressing the extra-stresses $\sigma_{zz} - \sigma_{rr}$ due to the polymer. The FENE-CR constitutive equations are adopted in this work [10]. In this approach, the polymer contribution is described by a Finitely Extensible Nonlinear Elastic (FENE) dumbbell model which makes use of the conformation tensor $\mathbf{A}$, and the stress tensor. For the one-dimensional model in dimensionless form, we obtain:

$$\sigma_{zz} = \tilde{G} f(R)(A_{zz} - 1),\ \sigma_{rr} = \tilde{G} f(R)(A_{rr} - 1) \quad (10)$$

$$R = \mathrm{tr}(\mathbf{A}) = A_{zz} + 2A_{rr} \quad (11)$$

where $\tilde{G} = \tilde{\nu}_p / D_e$, is the elastic modulus, and ν_p the polymer contribution to the viscosity and De=λ/τ, with λ the relaxation time. $f(R)$ is the finite extensibility factor related to the finite extensibility parameter L, representing the ratio of a fully extended polymer (dumbbell) to its equilibrium length:

$$f(R) = \frac{1}{1 - R/L^2} \quad (12)$$

L can be described in terms of molecular parameters, and is computed to be close to 15 for the polymer used in this study [2]. This latter value is adopted in the computations which have been performed.

The evolution equations for the conformation tensor **A** may be written as follows:

$$\frac{\partial A_{rr}}{\partial t} + v\frac{\partial A_{rr}}{\partial z} + \left(\frac{f(R)}{D_e} + \frac{\partial v}{\partial z}\right)A_{rr} = \frac{f(R)}{D_e} \quad (13)$$

$$\frac{\partial A_{zz}}{\partial t} + v\frac{\partial A_{zz}}{\partial z} + \left(\frac{f(R)}{D_e} - 2\frac{\partial v}{\partial z}\right)A_{zz} = \frac{f(R)}{D_e} \quad (14)$$

Results and discussion

Stretching: mid-filament diameter & transient profiles

Filament stretching simulations of the non-Newtonian polymer solutions, given in Table 1, for a stretching distance of 0.8mm (or aspect ratio L_f/R_0=2.3), using the FENE-CR constitutive equations have been performed. The mid-filament evolution results from numerical simulations are compared against experimental measurements (Fig. 4 and Fig. 5). Experimentally, the mid filament initially thins linearly with time after the piston cessation of motion indicating a viscous driven thinning mechanism [11, 12]. For polymer solutions, a sudden change occurs within the mid-filament in the form of an exponential decay characteristic of an elasto-capillary driven thinning mechanism. However we observe that near breakup a difference exists between the experimental and numerical mid-filament evolution of the polymer solution (Fig. 5). This difference is translated by an under-swelling observable in the numerical simulations only. Such a discrepancy may be attributed to the FENE-CR single mode model which is unable to fully describe the thinning of ultra dilute polymer solution, especially at the latest stages before filament breakup. Nevertheless, it is to be noted that the model, although not fully satisfactory, retrieves quiet well the main feature of the transient profiles, as for example the nascent bead (Fig. 4b and Fig. 5b). It also renders very well the break-up time of both Newtonia5n and polymeric fluids as shown below in Figure 5.

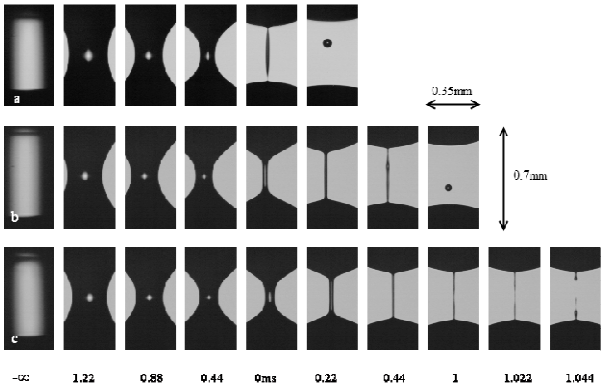

Figure 4. *Photographs of transient profile of filament thinning and break up experiments for matched viscosity samples of (a) Fluid I, (b) Fluid II and (c) Fluid III. Initial gap size: 0.6mm, final gap size: 1.4mm, pistons relative velocity: 150mm/s. Frame rate: 45000fps, shutter time of 3 μs. The reference time t = 0 has been chosen to be the Newtonian break up time.*

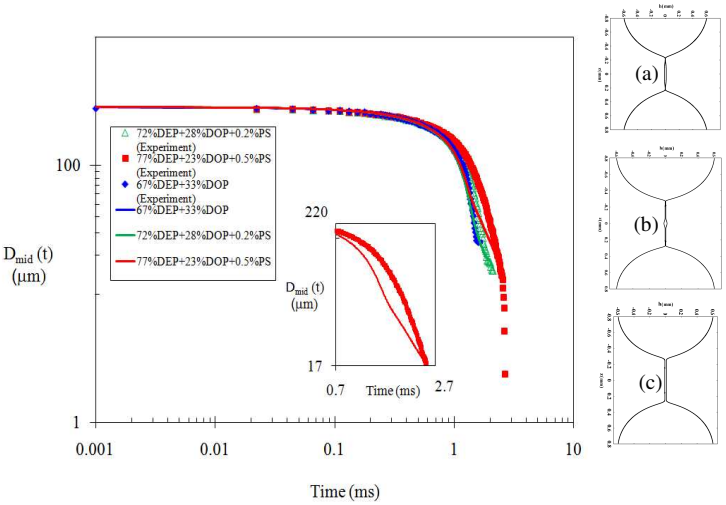

Figure 5. *Evolution of the mid-filament thinning diameter $D_{mid}(t)$ as a function of time for Fluid I, Fluid II and Fluid III. The insert highlights the discrepancy between the experimental and numerical mid-filament evolution. The left-hand figures shows the transient thinning profiles near breakup for fluids (a) I, (b) II, and (c) III, these figures are to be compared with those given above in Fig. 4.*

Pendant drop: transient profiles

The numerical modeling of a pendant drop is carried out both with the Newtonian and polymer fluids. Although these solutions have the same zero shear viscosity, a substantial difference may be drawn between them in terms of dripping faucet. The sequence of images of pendant drops for the three different fluids is shown in Figure 6. It may be noted that the addition of minute quantities of polymer leads, as expected, to long lasting filaments connecting the main drop to the nozzle.

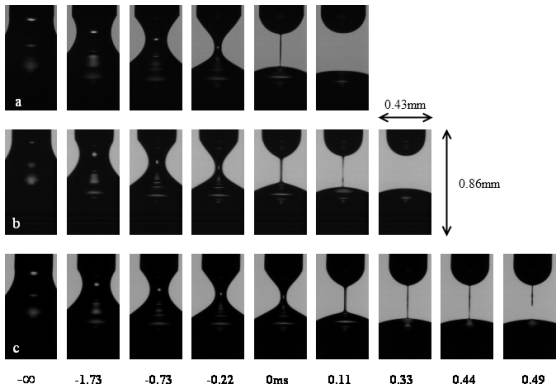

Figure 6. *Photographs of the pendant drop transient profiles for matched viscosity samples for (a) Fluid I, (b) fluid II and (c) Fluid III. Frame rate: 45000fps, shutter time of 3µs.*

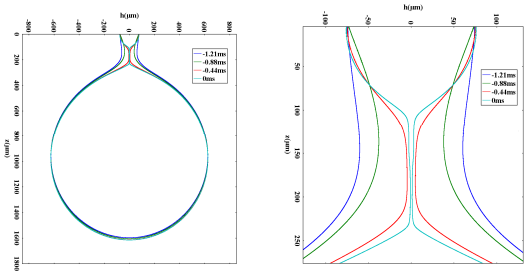

Figure 7. *Simulated pendant drop transient profile for Fluid I and close-up view.*

Such a behavior is retrieved by the numerical model where the transient profiles are in good agreement with the experimental ones. The Newtonian (Fluid I) case is particularly well predicted with the pinch-off point near the main drop (Fig. 7). In the polymer solution cases (Fluids II and III), we also observe a quite good prediction of the filament length (Fig. 8).

To the best of our knowledge this is the first time that the pendant drop problem of non-Newtonian fluids is fully addressed using the one dimensional approach. This opens the way for sensitivity studies as the one performed in the following section since the numerical cost of such an approach could be one to two orders of magnitude smaller than the CPU time required by the 2D computations on the same machine.

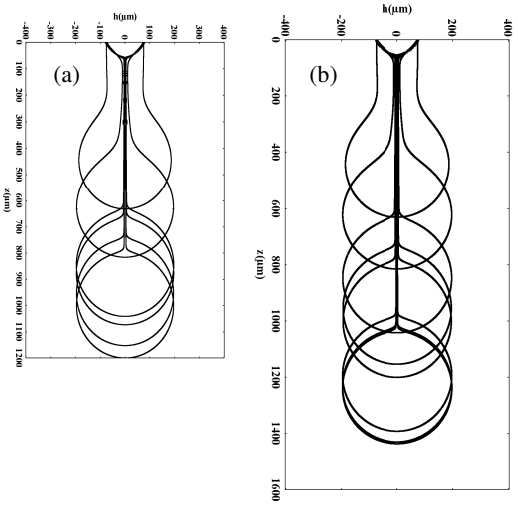

Figure 8. *Transient profile of the pendant drop in the case of non-Newtonian polymer solutions (a) Fluid II and (b) Fluid III.*

Printing behavior

We investigate here the printing behavior of a DOD piezoelectric ink-jet printer in order to propose a printability criterion. It is used to carry out the ejection of drops formed with fluids I, II, and III (Fig.9). It is well known that droplet formation is very much influenced by the system's response to an applied pressure stimulus on the fluid. The printer used in the present study has a nozzle of 30 µm and the ejection pulse width is around 8 µs.

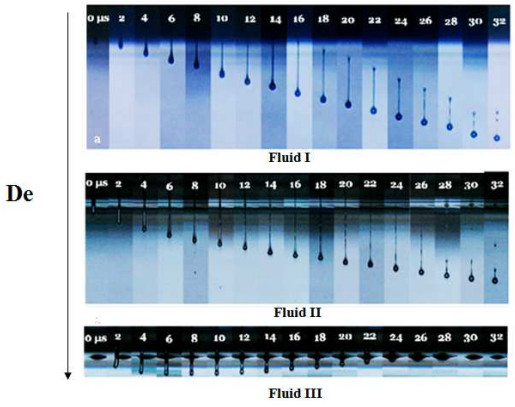

Figure 9. *Drop formation for the different fluids described in table 1.*

It is shown that the fluids I and II may be ejected, although with different filament lengths, and that fluid III shows an anomalous "sticking" behavior. The drop begins to form but after some time is drawn back into the nozzle. This is probably related to the fact that a typical voltage wave form consists of a positive pulse (dwell time) generally followed by a negative pulse (echo time). The amplitude of the pulse and its duration is not sufficient to form fully the filament and eject the drop in the case of fluid III.

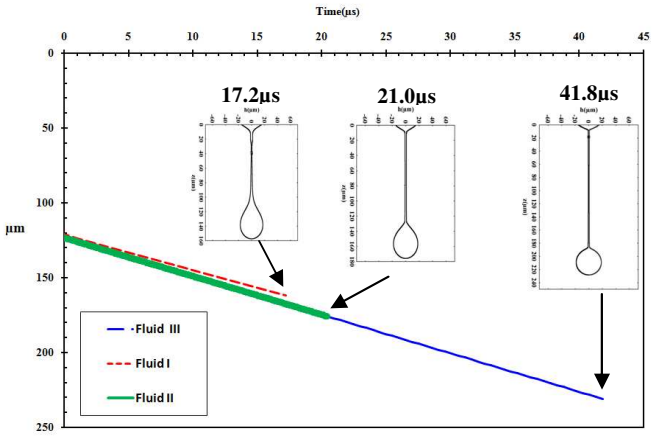

Figure 10. *Simulated profiles and break-up lengths for the three different fluids described in Table 1.*

The numerical investigation performed with the 1D model reveals some interesting features (Fig.5). The comparisons between experiments and simulations are made relatively to the Newtonian fluid. In the case of the lower viscoelastic fluid (Fluid II) the break-up occurs at a time of 21 µs in very agreement with the results obtained experimentally. The simulations also give the length of the filament at break-up which is around 175 µm and only about 15 µm longer than that of the Newtonian fluid. The length of the filament the higher viscoelastic fluid (Fluid III) is much longer (230 µm) and most importantly break-up occurs much later with the break-up time being almost 2.5 times that of the Newtonian fluid. Any negative pulse sent to the transducer before break-up of the filament would probably tend to draw back the fluid to the nozzle which is indeed seen experimentally (Fig. 9). Numerical simulations taking into account the oscillatory nature of the flow with positive and negative pulses are currently underway and will be reported.

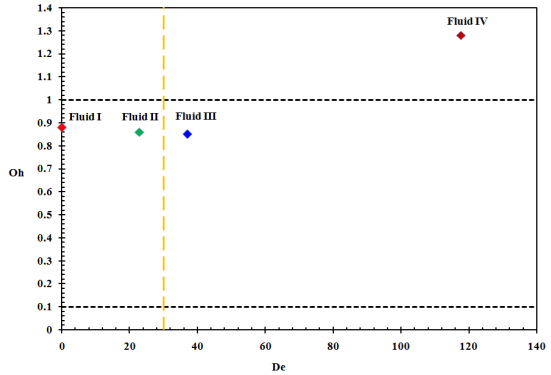

Figure 11. *Oh-De diagram with the boundaries of the printing domain (---). Fluids I, II, III and IV are on spotted on the figure.*

Figure 11 is a first step towards defining a printing domain in the case of viscoelastic fluids. Even if fluids I, II and III satisfy the double condition of 0.1<Oh<1 and of We=11 >1 [1, 13], the addition of polymer leads to a long lasting filament which hinders printing with fluid III. The viscoelastic character of the fluid is manifested through the Deborah number De. This work shows that this number should be smaller than 30 for the fluid to be printable without too many restrictions. Drop formation with fluid III is hindered because of the Deborah number being higher than 30 whilst fluid IV suffers from two drawbacks with $Oh_{IV} > 1$ and De_{IV} almost 4 times the critical Deborah number. It has been shown experimentally that this fluid cannot be ejected.

Conclusion

In this paper experiments and numerical simulations are performed for filament thinning, pendant drop and DOD processes. A comparison between the first two configurations shows the same behavior which highlights the relevance of the stretching device for characterizing extensional flow and in particular DOD printing. In order to address these issues a 1D model based on a FENE-CR single mode constitutive equation has been developed and shown to represent fairly well the behavior of dilute viscoelastic polymer solutions in a number of free-surface flows and namely DOD printing. The versatility of this model is finally used to perform sensitivity studies and define a printing domain taking into account the Ohnesorge and Deborah numbers. As such, it paves the way for optimized printing with both Newtonian and non-Newtonian fluids.

Acknowledgements

MT and AS wish to acknowledge financial support from ANR PAN'H 2008 CATIMINHY project. DV wishes to thank the Engineering and Physical Sciences Research Council (UK) and industrial partners in the Innovation in Industrial Inkjet Technology project, EP/H018913/1 for financial support.

References

[1] B. Derby, "Inkjet printing of functional and structural materials fluid property requirements, feature stability and resolution", Ann. Rev. Mater. Res. 40, 395-414, (2010).

[2] M. Tembely, D. Vadillo, M.R. Mackley and A. Soucemarianadin "The matching of a "one-dimensional" numerical simulation and experiment results for low viscosity Newtonian and non-Newtonian fluids during filament stretching and break up", Journal of Rheology, (2011) (*submitted*).

[3] D.C. Vadillo, T. R. Tuladhar, A. Mulji, M.R. Mackley, "The Rheological characterisation of linear viscoelasticity for ink jet fluids using a Piezo Axial Vibrator (PAV) and Torsion Resonator (TR) rheometers", J. Rheology, 54(4), 781-79 (2010).

[4] D.C Vadillo, T.R. Tuladhar, A.C. Mulji, S. Jung, S.D. Hoath, M.R. Mackley, "Evaluation of the inkjet fluid's performance using the "Cambridge Trimaster" filament stretch and break-up device", J. Rheology, 54(2), pp. 261-282, (2010).

[5] V. Tirtaatmadja, G.H. McKinley, J.J Cooper-White, "Drop formation and breakup of low viscosity elastic fluids: effects of molecular weight and concentration" Physics of Fluids, 18, (2006).

[6] J. Eggers, "Nonlinear dynamics and breakup of free-surface flows", Rev. Mod. Phys., 69, 865-929 (1997).

[7] C. Clasen, J. Eggers, M. A. Fontelos, J. Li, G. H. McKinley, "The beads-on-string structure of viscoelastic threads", J. Fluid Mech. 556, 283, (2006).

[8] D.T. Papageorgiou, "Analytical description of the breakup of liquid jets", J. Fluid Mech. 301, 109, (1995).

[9] M. A. Fontelos and J. Li, "On the evolution and rupture of filaments in Giesekus and FENE models", J. Non-Newtonian Fluid Mech. 118, 1-16, (2004).
[10] M. D. Chilcott and J. M. Rallison, "Creeping flow of dilute polymer solutions past cylinders and spheres", J. Non-Newtonian Fluid Mech. 29, 381-432, (1988).
[11] R. F. Liang and M. R. Mackley, "Rheological characterization of the time and strain dependence for polyisobutylene solutions", J. Non Newtonian Fluid Mech. 52, pp. 387-405, (1994).
[12] V.M. Entov and E.J. Hinch, "Effect of a spectrum relaxation times on the capillary thinning of a filament elastic liquids", J. Non-Newtonian Fluid Mech., 72, 31-53 (1997).
[13] N. Reis, B. Derby "Ink jet deposition of ceramic suspensions: modelling and experiments of droplet formation". MRS Symp. Proc. 624:65–70, (2000).

Author Biography

Dr Moussa TEMBELY received his PhD in Fluid Mechanics from the University of Grenoble, France, in 2010. He also holds a MSc. from the French aerospace engineering school, SUPAERO. His background is in fluid and solid dynamics, and his research interests include droplet dynamics, fluid instability, fluid-structure interaction, inkjet printing, spray generation, heat transfer, fuel cell modeling, as well as computational fluid dynamics. He is currently a postdoctoral research fellow in the group of Prof. A. Soucemarianadin at the Laboratory for Geophysical and Industrial Flow Research (LEGI), Grenoble, France.